

Isomers of β -substituted di and tri-nitrotetraphenylporphyrins and their copper(II) derivatives: Structure, optical and electrochemical redox properties

S DAHAL, V KRISHNAN* and M NETHAJI

Department of Inorganic and Physical Chemistry, Indian Institute of Science, Bangalore 560 012, India

Also at Jawaharlal Nehru Centre for Advanced Scientific Research, Indian Institute of Science Campus, Bangalore 560 012, India

MS received 13 October 1997

Abstract. Controlled nitration of *meso*-tetraphenylporphyrinatocopper(II) using fuming nitric acid leads to the formation of different β -substituted nitro derivatives. Five isomers of dinitro and three isomers of trinitrotetraphenylporphyrins have been isolated and characterised using FAB/MS, ^1H NMR, UV-VIS and IR spectroscopies. The single crystal X-ray data on the copper(II) derivative of one of the isomers of trinitrotetraphenylporphyrin revealed 'saddle' conformation of the porphyrin core resulting from the nitro group substitution at the β -pyrrole carbons. The electrochemical redox behaviour of the free-base porphyrins and their copper(II) derivatives revealed that successive substitution of nitro groups at the pyrrole carbons shifts the one-electron ring oxidations anodically while the ring reduction occurs at a less cathodic potential relative to the unsubstituted porphyrin. The isomer specific shifts in the redox potentials bear a direct relationship with the relative energy levels of HOMO/LUMO obtained from AM1 calculations.

Keywords. Isomers; di and trinitrotetraphenylporphyrins; ring-redox potentials; crystal structure; trinitrotetraphenylporphyrinatocopper(II).

1. Introduction

The tetrapyrrole pigments play an important role in photosynthetic and respiration processes. Among the many model compounds to biomimic these processes, mesotetraphenylporphyrin (H_2 TPP) and its derivatives form the most versatile systems. Porphyrins bearing different substituents have attracted wide attention in view of their novel structures and reactivity patterns¹⁻⁴. It has recently been shown that the nitro groups substitution at the pyrrole carbons leads to the exhibition of intramolecular charge transfer⁵ substituent induced saddling of the porphyrin core⁶, improved catalytic activity⁷ and newer routes for the synthesis of functionalised porphyrins⁸⁻¹⁰. There have been many attempts to obtain polynitro substituted porphyrins in the literature⁷⁻¹¹, however in most of these procedures, no characterisation of specific isomers of these derivatives has been reported and studied. It is recognised that isolation and evaluation of different properties of these isomers provide important information on the structure-reactivity relationship in these systems which is of interest towards understanding of biofunctions. Here, a simple and elegant method to obtain

*For correspondence

five isomers of dinitro- and three isomers of trinitro-tetraphenylporphyrins (figure 1) exhibiting unusual imino proton tautomerism and interesting structural, optical and electrochemical properties are described.

2. Experimental

The free-base dinitro and trinitrotetraphenylporphyrins were prepared by the nitration of 5, 10, 15, 20-tetraphenylporphyrinatocopper(II), CuTPP followed by acid demetallation. The strategy adopted is to carry out nitration by the controlled addition of a calculated amount of freshly distilled fuming nitric acid to a solution of the porphyrin dissolved in organic solvent.

2.1 Preparation of 2, 12 (*a*) and 2, 13 (*b*) dinitrotetraphenylporphyrin

CHCl_3 solution containing 100 mg of CuTPP (in 100 ml) was gently stirred with the dropwise addition of 0.70 ml of fuming nitric acid at a constant rate over a period of 1.2 min. It was then immediately neutralised with an aqueous NaOH solution. The organic layer was then dried over anhydrous sodium sulphate and the solvent was removed under reduced pressure. The brownish red product was then chromatographed on a basic alumina column using CHCl_3 /Pet.ether (2:1, v/v) as the eluant. Demetallation was achieved by dissolving the purified product in a minimum amount of concentrated sulphuric acid followed by slow addition to an uniformly stirred ice-cold concentrated ammoniacal solution. The product was dissolved in CHCl_3 and thoroughly washed with water. The organic layer was dried over anhydrous sodium sulphate. The product was initially purified by column chromatography and finally by repetitive thin layer chromatographic method. Silica gel (TLC grade) was used as the absorbent material. The eluant used was CHCl_3 :Pet.ether (20/80, v/v). Two closely separated bands of brownish yellow colour were obtained with relative R_f value of 1.00:0.94. The two bands were separately collected and the compound extracted with CHCl_3 . The yield was $\approx 20\%$ calculated with respect to the amount of starting material (CuTPP) used. A small amount of mono-nitro derivative and other dinitro derivatives were also formed during the reaction.

The FAB mass spectra ($m/e = 705$) agree well with the calculated mass of the derivatives (calc. $m/e = 704.7$). Infrared analysis confirmed the presence of nitro group in both the derivatives with the appearance of characteristic strong frequency at 1341–1347 and 1527–1532 cm^{-1} . ^1H NMR spectral data in CDCl_3 at 298 K, δ in ppm (nature of resonance, number of protons, J in Hz): Isomer *a*: 9.01 (s, 2), 9.02 (d, 1, $^4J = 1.80$), 9.00 (d, 1, $^4J = 1.83$), 8.95 (d, 1, $^4J = 1.88$), 8.92 (d, 1, $^4J = 1.80$), 8.34–8.19 (m, 8), 7.92–7.65 (m, 12), –2.58 (bs, 2); Isomer *b*: 9.02 (s, 2), 8.93 (bs, 4), 8.29–8.19 (m, 8), 7.84–7.72 (m, 12), –2.48 (bs, 1), –2.57 (bs, 1).

2.2 Preparation of 2, 8 (*c*), 2, 7 (*d*) and 3, 7 (*e*) dinitrotetraphenylporphyrin

The synthetic procedure employed was the same as outlined above except for the amount of fuming nitric acid added (1.0 ml) and the duration of addition (1.0 min). The product was purified on a basic alumina column using CHCl_3 /Pet. ether (70:30, v/v) as the eluant. The product was demetallated by using a similar procedure as described above. The product was initially purified by column chromatography and finally by repetitive TLC using CHCl_3 /Pet. ether (30:80, v/v) as the eluant. Three major green

coloured bands were observed with a relative R_f value of 1.00:0.93:0.82. The yield of the pure product was 20% of the starting material (CuTPP). Trace amounts of isomers a, b and trinitro derivatives were also formed during the reaction.

The FAB mass spectra ($m/e = 705$) agree well with the calculated mass of the derivatives (calc. $m/e = 704.7$). The IR spectra of the three derivatives confirmed the presence of the nitro group. $^1\text{H NMR}$ spectral data in CDCl_3 at 298 K, δ in ppm (nature of resonance, number of protons, J in Hz): Isomer c: 9.06 (s, 2), 8.82 (d, 2, $^3J = 4.96$), 8.72 (d, 2, $^3J = 4.96$), 8.21 – 8.17 (m, 8), 7.85 – 7.68 (m, 12), –2.11 (bs, 2); Isomer d: 9.04 (s, 1), 9.03 (s, 1), 8.86 – 8.73 (m, 4), 8.26 – 8.18 (m, 8), 7.81 – 7.73 (m, 12), –2.18 (bs, 2); Isomer e: 8.98 (s, 2), 8.80 (d, 2, $^3J = 4.86$), 8.76 (d, 2, $^3J = 4.90$), 8.30 – 8.15 (m, 8), 7.85 – 7.64 (m, 12), –2.26 (bs, 2).

2.3 Trinitrotetraphenylporphyrin derivatives

The trinitro derivatives of H_2 TPP were prepared using a similar procedure outlined for the dinitro derivatives except that 2.0 ml of fuming nitric acid was used for the nitration experiments. The period of reaction was maintained at 1 min. The neutralised product was purified on a basic alumina column using CHCl_3 :Pet.ether (70:30, v/v) as the eluant. Demetallation was achieved using a procedure similar to that described for the dinitro derivatives. The product was initially purified on a basic alumina column and finally purified by repetitive TLC employing CHCl_3 /Pet.ether (30:70, v/v) as the eluant. Three major green bands were observed with relative ratio of R_f values for the isomers, a:b:c as 1.00:0.90:0.80. A small amount of dinitro derivatives were also formed during the course of the reaction. The yield of the isomeric mixture of trinitro derivative was 15% of the amount of CuTPP used for the reaction.

The mass spectra of all the derivatives with m/e peak at 750 agree well with the calculated values of trinitrotetraphenylporphyrin (calc. $m/e = 749.74$). The IR spectra confirms the presence of the nitro group. $^1\text{H NMR}$ spectral data in CDCl_3 at 298 K, δ in ppm (nature of resonance, number of protons, J in Hz): Isomer f: 9.09 (bs, 1), 8.94 (s, 1), 8.89 (bs, 2), 8.86 (s, 1), 8.83 – 8.20 (m, 8), 7.97 – 7.50 (m, 12), –1.99 (bs, 2); Isomer g: 9.05 (bs, 1), 8.96 (d, 1, $^3J = 5.14$), 8.84 (bs, 1), 8.30 – 8.24 (m, 8), 7.90 – 7.69 (m, 12), –2.11 (bs, 2); Isomer h: 8.97 (bs, 1), 8.93 (s, 1), 8.90 (bs, 2), 8.85 (s, 1), 8.34 – 8.18 (m, 8), 7.87 – 7.67 (m, 12), –2.12 (bs, 2).

2.4 Preparation of copper (II) derivatives of the di and trinitrotetraphenyl porphyrin

The copper (II) derivatives of the nitro porphyrins were prepared from the purified isomers using a procedure described in literature ¹². Recrystallised copper (II) acetate dissolved in CH_3OH was added to the free-base porphyrin dissolved in chloroform. The mixture was refluxed for one hour to ensure complete metallation. the product was then washed with hot water several times and the organic layer was dried over anhydrous sodium sulphate. The compound was purified on a basic alumina column using CHCl_3 : Pet.ether (80:20, v/v) as the eluant.

2.5 Methods

The optical spectra were recorded on instruments described earlier ¹³. The cyclic voltammograms and differential pulse voltammetry of the free-base porphyrins and their copper (II) derivatives in CH_2Cl_2 were recorded on a BAS-100A Electrochemical analyser. A three electrode assembly consisting of gold working electrode, platinum

wire auxillary electrode and a saturated calomel electrode were used for redox potential measurements. Tetrebutylammoniumhexafluorophosphate was used as the supporting electrolyte.

2.6 Single crystal X-ray data

Purple rectangular plates of 3, 7, 13 trinitro 5, 10, 15, 20-tetraphenylporphyrinatocopper(II) were grown from a saturated $\text{CHCl}_3/\text{CH}_3\text{OH}$ solution at 25°C by slow evaporation and a crystal of dimension $0.070 \times 0.095 \times 0.165$ mm was used for data collection. 25 reflections in the range $8.5 < \theta < 13.6$ were used for cell determination and intensity data was collected in the range $1 < \theta < 20$. No significant intensity decay was observed. The data were corrected for Lorentz and polarisation effects and not for absorption. Other details of data collection are summarised in table 1. The structure was solved by direct methods using SHELXS-86 program¹⁴ which revealed the positions of all the non-hydrogen atoms of the porphyrin core and the phenyl groups. Subsequently, the positional parameters of all other atoms were identified from

Table 1. Crystal data of isomer 3, 7, 13 trinitro copper(II) tetraphenylporphyrin

$\text{C}_{44}\text{H}_{25}\text{CuN}_7\text{O}_6$	MoK α radiation
$M_r = 811, 25$	$\lambda = 0.71609 \text{ \AA}$
Triclinic	Cell parameters from 25 reflections
$P\bar{1}$	$\theta = 2.0 - 22.0^\circ$
$a = 10.647(7) \text{ \AA}$	$\mu = 0.68 \text{ mm}^{-1}$
$b = 13.720(7) \text{ \AA}$	$T = 295 \text{ K}$
$c = 14.531(6) \text{ \AA}$	Cubic
$\alpha = 62.76(4)^\circ$	$0.165 \times 0.10 - 0.057 \text{ mm}$
$\beta = 79.66(4)^\circ$	Bluish green
$\gamma = 69.11(3)^\circ$	Crystal source: slow evaporation
$V = 1763(2) \text{ \AA}^3$	from $\text{CH}_2\text{Cl}_2/\text{CH}_4\text{O}$ solution
$Z = 2$	
$D_x = 1.528 \text{ Mg M}^{-3}$	
<i>Data collection</i>	
Enraf-Nonius CAD-4 diffractometer	$R_{int} = 0.0231$
w/2 θ scans	$\theta_{max} = 20^\circ$
Absorption correction: none	$h = 0 \rightarrow 11$
8196 measured reflections	$k = -13 \rightarrow 14$
4319 independent reflections	$l = -15 \rightarrow 15$
1720 observed reflections	3 standard reflections
$I_0 > 2.5\sigma(I_0)$	frequency: 60 min
	intensity variation: < 10%
<i>Refinement</i>	
Refinement on F^2	$(\Delta/\sigma)_{max} = 0.33$
$R = 0.1134$	$\Delta\rho_{max} = 0.53 \text{ e \AA}^{-3}$
$wR(F^2) = 0.3834$	$\Delta\rho_{min} = -0.46 \text{ e \AA}^{-3}$
$S = 1.727$	Extinction correction: none
1720 reflections	Atomic scattering factors
523 parameters	from SHELX93
H atoms refined as riding	$w = 1/[\sigma^2(F_0^2) + (0.1P)^2]$
with common isotropic H	where $P = (F_0^2 + 2F_c^2)/3$

difference maps. The structures were refined using SHELXL-93¹⁵ assigning anisotropic thermal parameters. The hydrogen atoms were placed on the geometrically calculated positions and allowed to ride, during refinement, on the atoms to which they are attached. The refinement in SHELXL-93 is based on F^2 and was carried out with all reflection having positive values for F^2 in order to increase the reflections to parameters ratio. Other details such as final R factors, goodness of fit and the features of final difference map are listed in table 1.

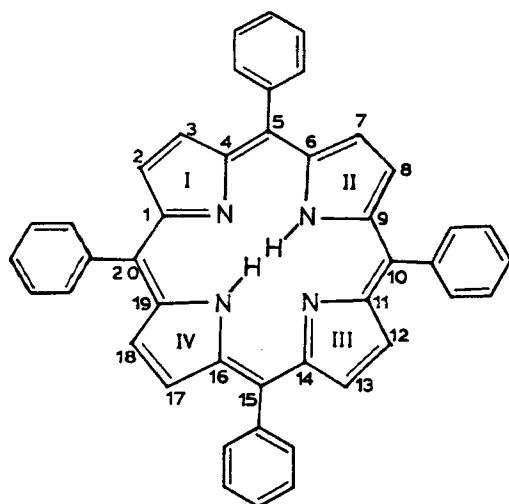
3. Results and discussion

Polynitration of the H_2 TPP can, in principle, lead to nitration of all the eight β -pyrrole carbons and the four phenyl groups. It is seen that under the present experimental conditions, only the β -pyrrole substituted nitro porphyrins are being formed. Nitration at β -pyrrole position should give rise to six isomers of dinitro derivative and six isomers of trinitro derivative. However, in the present study only five isomers of dinitro and three isomers of trinitrotetraphenylporphyrin were isolated (figure 1). The isomers bearing two nitro groups in the same pyrrole ring were not isolated. The different isomers of the nitro derivatives were characterised by 1H NMR, UV-VIS spectral methods and also supported by single crystal data wherever possible.

3.1 1H NMR studies

The 1H NMR spectra of the free-base porphyrins are highly characteristic of the position of nitro group substitution and establish the structural integrity of the compounds. The integrated intensity of the resonances agree well with the number of protons. The assignment of various resonances is carried out by comparison with the 1H NMR spectra of the unsubstituted derivative H_2 TPP.

Variable temperature 1H NMR and irradiation experiments (NOE) have been useful in arriving at the identity of the isomers. The pyrrole proton resonances of the isomer **a** is assigned to ABC type of spectrum where the lowest field signal (*A*) is assigned to the



Dinitro derivatives

a = 2, 12 = NO₂; 3, 7, 8, 13, 17, 18 = H

b = 2, 13 = NO₂; 3, 7, 8, 12, 17, 18 = H

c = 2, 8 = NO₂; 3, 7, 12, 13, 17, 18 = H

d = 2, 7 = NO₂; 3, 8, 12, 13, 17, 18 = H

e = 3, 7 = NO₂; 2, 8, 12, 13, 17, 18 = H

Trinitro derivatives

f = 3, 7, 12 = NO₂; 2, 8, 13, 17, 18 = H

g = 3, 7, 13 = NO₂; 2, 8, 12, 17, 18 = H

h = 2, 7, 13 = NO₂; 3, 8, 12, 17, 18 = H

Figure 1. Isomers of di- and tri-nitrotetraphenylporphyrin.

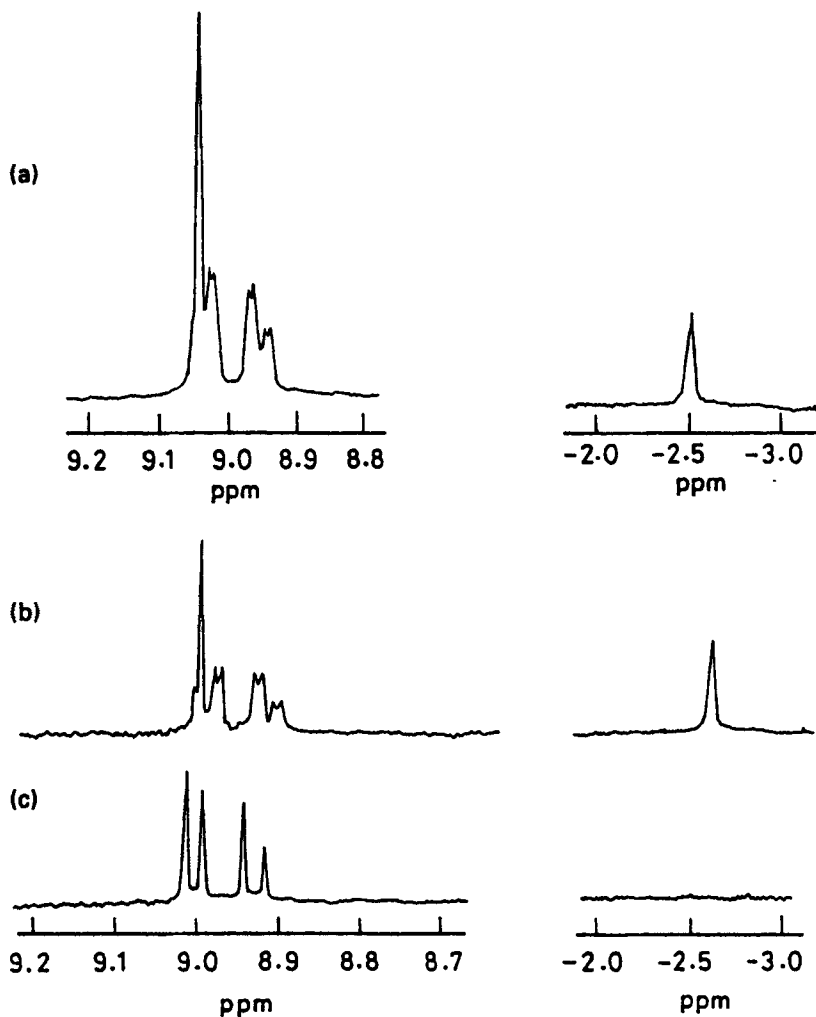


Figure 2. The ^1H NMR spectrum of free-base 2,12-dinitrotetraphenylporphyrin (a) at 298 K (b) at 228 K and (c) irradiation at of N-H proton at -2.54 ppm in CDCl_3 .

protons adjacent to the nitro groups of the pyrrole rings. The higher field signals *B* and *C* appear as two doublets due to ^3J coupling ($^3\text{J} = 5.10$ Hz). The two doublets are further split by ^4J coupling ($^4\text{J} = 1.80$ Hz) with imino protons giving rise to four doublets. In the spectrum of the isomer a, however, it is found that one of the doublets is merged with the proton of resonance of *A* (lower field). The above assignments and the position of nitro groups in different pyrrole rings can be easily found out by irradiation experiments. Irradiation at the imino proton signal of the isomer a at room temperature leads to the collapse of the doublets (arising from ^4J coupling) into a singlet (figure 2). The irradiated spectrum displays a singlet (arising from *A* protons) and two doublets ($^3\text{J} = 5.10$ Hz), one of the signals of the doublet being merged with the proton signal of *A*. The *A* proton resonance remains unchanged before and after irradiation.

This leads to the suggestion that the imino protons are not located in the pyrrole rings bearing nitro groups and are predominantly situated at the nitrogens of the pyrrole rings bearing no nitro group.

It is of interest to note that in isomer **b**, the imino protons occur as two singlets at room temperature and lowering of temperature results in the separation of two singlets rather than appearance of any multiplet. However, on increasing the temperature above the ambient temperature, the two singlets merged to a singlet. This observation suggests the possibility of coexistence of two tautomers and fast equilibrium at high temperature or the differing electron densities at the nitrogens that bear the protons. The β -pyrrole proton resonances arising out of isomer **b** at room temperature can be classified as AB type. The lower field signal arising from A protons while large broadening of B proton signal is observed. On lowering of temperature the AB type of spectrum transfers to ABC type with 4J coupling similar to that observed for room temperature spectra of the isomer **a**. Irradiation of the imino resonances at low temperature leads to the collapse of the doublets of B and C protons and the resonance of A proton remains unaffected. This suggests that the imino protons are localised at the opposite pyrrole rings that do not bear the nitro groups. There is a strong indication that there exists only one tautomer and the appearance of two imino proton signals of isomer **b** arise essentially from the differing electron densities on the nitrogens. The assignment of the specific position of nitro groups amongst the isomers **a** and **b** is easily arrived at from the simple 1H NMR spectra of the zinc(II) complexes of these isomers without the imino proton coupling with β -pyrrole proton resonances. The pyrrole proton resonances of zinc(II) complex of isomer **a** exhibits ABC type of spectrum. The A type corresponds to two protons and appears as a singlet resonance in the lowest field of the spectrum. The B and C type corresponding to two protons each, appear as doublets ($^4J = 5-10$ Hz). The isomer **Znb** exhibits ABB' type of spectrum for the pyrrole proton resonances. The B and B' type appear as two closely placed singlets corresponding to two protons each. It is seen that the substitution at 3, 13 positions of the porphyrin ring would give rise to ABC type of spectrum while substitution at 3, 12 positions should give ABB' type of spectrum. This is substantiated by the X-ray crystal structure of the isomer **b** wherein the nitro groups are positioned in 3, 12 positions of the porphyrin ring ⁶.

The pyrrole proton resonances of the isomers **c**, **d** and **e** are clearly distinguishable as revealed from the nature of the multiplets. Thus, isomer **c** and **e** exhibit ABC type of resonances, while a ABB'CD type was observed for isomer **d** for the pyrrole proton resonances. This observation leads to the suggestion of location of nitro groups at the adjacent pyrrole rings of the porphyrin. In addition, lowering the temperature to 228 K results in the broadening of all the pyrrole proton resonances. Interestingly broadening of these resonances is accompanied with the appearance of two distinct imino proton resonances for isomer **e** while no change is observed for this resonance in isomers **c** and **d**. These observations coupled with the differing magnitude of separation of the doublets permit the characterisation of these isomers, wherein the nitro groups are located in different pyrrole carbons.

The five pyrrole proton resonances of trinitrotetraphenylporphyrins appear as singlets and doublets depending on the locations of nitro groups in the different pyrrole rings. It is easier to analyse the pyrrole proton resonances in the different isomers using the following reasons. The appearance of doublet resonance for unsubstituted pyrrole protons in the trinitro isomers suggests asymmetric disposition of nitro groups in the adjacent pyrrole rings with respect to the unsubstituted pyrrole rings;

while a symmetric disposition leads to the display of singlet resonance for pyrrole protons. Interestingly, the protons located in the unsubstituted pyrrole ring resonate at a lower field relative to one of the proton resonances of substituted pyrrole ring. This arises from the favoured path of the ring current in these porphyrins¹⁶. Support for this assignment comes from the ¹H NMR spectra of the corresponding zinc (II) complexes wherein the favoured path of ring current is absent. Here, the protons of the unsubstituted pyrrole rings resonate at a relatively higher field with respect to the proton resonances of the substituted pyrrole rings. At room temperature isomers **f** and **h** exhibit four singlet resonances while isomer **g** displays three singlet and two doublet resonances for the pyrrole protons. On lowering of temperature (228 K), it is found that all the pyrrole proton resonances are shifted to a lower field accompanied by large broadening and in some cases splitting of the ⁴J coupled pyrrole protons. At 228 K isomer **f** exhibits four imino proton resonances at -1.90, -1.96, -2.02 and -2.12 ppm arising from the presence of two tautomers. The major tautomer (> 80%) has been identified as that which exhibits -NH resonances at -1.90 and -1.96 ppm based on the relative intensity of the signals. It is of interest to note that isomers **g** and **h** exhibit only two imino proton resonances. Irradiation experiments performed on these isomers reveal that in case of isomer **f**, the major tautomer has imino protons located on the opposite pyrrole rings, one of which is unsubstituted. The presence of only one tautomer is found in isomer **g** and **h** wherein the imino protons favours the pyrrole ring which is unsubstituted. Typically in case of isomer **f** at 228 K the pyrrole proton resonances occur at 9.18 (d, 1, ⁴J = 2.08 Hz), 9.02 (s, 1), 8.99 (bs, 2) and 8.95 (s, 1) ppm. Irradiation at -1.90 ppm leads to the collapse of the doublet at 9.18 ppm into a singlet accompanied by a large increase in the intensity of the resonance. Irradiation at -1.96 ppm leads to a large increase in intensity and narrowing of the peak at 8.99 ppm. These imino proton resonances correspond to the major tautomer, wherein the imino protons are present at the opposite pyrrole rings, one of which is unsubstituted. Irradiation at -2.02 and -2.12 ppm leads to a small increase in intensity of the part of the doublet resonance at 9.11 ppm and a slight increase in intensity of peaks at 9.02 and 8.95 ppm. The assignment of specific position of nitro groups has been further substantiated by the single crystal X-ray structure solved for the copper(II) derivative of isomer **g**.

3.2 Optical absorption studies

The UV-VIS spectral data of the copper(II) derivatives are presented in table 2. The optical spectral features of the free-base di- and tri-nitrotetraphenylporphyrins have earlier been discussed in terms of intramolecular charge transfer in their singlet excited states¹⁷. It is seen that the successive addition of nitro groups in the pyrrole carbons of the porphyrins shifts both the B and Q(0, 0) bands to the red region. The wavelength of the optical transitions follow the number of the nitro substituents as mono < di < tri. The same trend is followed in the spectral features of the free-base porphyrins and their zinc(II) derivatives. A possible reason for the observed shifts in the absorption bands can be understood in terms of the four orbital model of Gouterman¹⁸ (figure 3). The electronic structure of porphyrins can be described in terms of two occupied π -molecular orbitals (a_{2u} and a_{1u}) and unoccupied degenerate π -molecular orbitals (e_g). The perturbation of the relative energy levels of different isomers, as a consequence of symmetry lowering is investigated using AM1 calculations (CI = 5, involving 100

Table 2. Optical spectral data^a of copper(II) derivatives of the different isomers of di- and tri-nitrotetraphenylporphyrins in CH₂Cl₂ at 298 K

Isomers	B(0,0)(log ϵ)	Q(1,0)(log ϵ)	Q(0,0)(log ϵ)
Cu \underline{a}	435.0(5.00)	558.0(3.89)	602.2(3.78)
Cu \underline{b}	434.4(4.99)	559.9(3.88)	606.0(3.85)
Cu \underline{c}	438.7(5.04)	560.1(4.04)	
Cu \underline{d}	434.7(5.20)	558.5(4.03)	603.9(3.99)
Cu \underline{e}	439.8(5.05)	560.7(3.95)	607.0(3.80)
Cu \underline{f}	444.3(4.66)	570.8(3.57)	610.8(3.46)
Cu \underline{g}	442.6(4.65)	58.7(3.51)	612.6(3.45)
Cu \underline{h}	450.7(5.02)	574.0(4.01)	615.4(3.86)

^aAbsorption bands in nm. The log ϵ values are in parenthesis. The copper(II) derivative of mononitrotetraphenylporphyrin has absorption bands, 422.0 (5.26); 547.0 (4.11) and 582.0 (3.92)²³

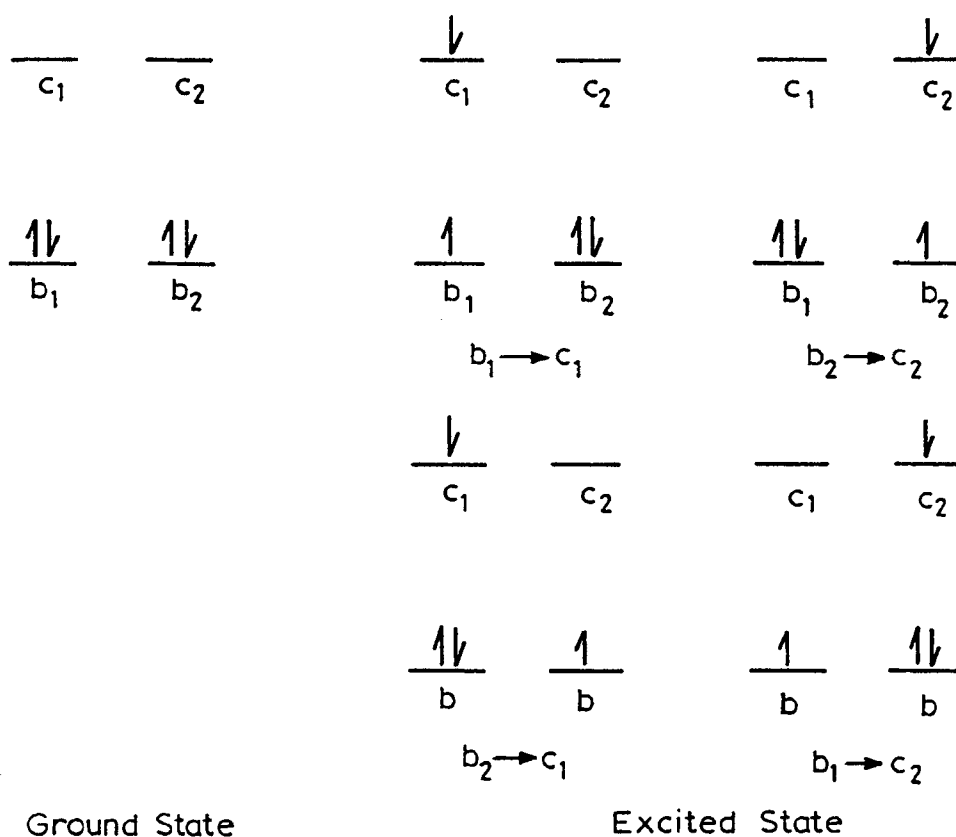
**Figure 3.** Schematic diagram of frontier orbital description of porphyrins.

Table 3. The one electron redox potentials of dinitro and trinitrophenylporphyrins in CH_2Cl_2 at 298 K

Isomer	$E_{1/2}^a$ (V)				
	Reduction			Oxidation	
	I $\text{P} \rightarrow \text{P}^{\cdot-}$	II $\text{P} \rightarrow \text{P}^{2-}$	III b	I $\text{P} \rightarrow \text{P}^{\cdot+}$	II $\text{P} \rightarrow \text{P}^{2+}$
<u>a</u>	-1.12	c	c	0.69	c
<u>Cua</u>	-1.226	-1.316	-1.525	0.713	1.065
<u>b</u>	-1.15	c	c	0.70	0.89
<u>Cub</u>	-1.215	-1.310	-1.515	0.717	1.070
<u>c</u>	-1.24	-1.47	1.76	0.69	0.87
<u>Cuc</u>	-1.284	-1.516	c	0.716	1.025
<u>d</u>	-1.20	-1.3	-1.82	0.70	c
<u>Cud</u>	-1.212	-1.364	c	0.716	1.075
<u>e</u>	-1.16	-1.29	-1.92	0.70	c
<u>Cue</u>	-1.261	-1.447	c	0.722	1.105
<u>f</u>	-1.12	-1.38	-1.61	0.77	c
<u>Cuf</u>	-1.086	-1.280	c	0.800	c
<u>g</u>	-0.98	-1.07	-1.65	0.73	0.91
<u>Cug</u>	-1.071	-1.277	c	0.800	c
<u>h</u>	-1.01	-1.13	-1.61	0.75	c
<u>Cuh</u>	-1.090	-1.328	c	0.805	c

^aThe potentials are referred against Fc/Fc^+ couple

^bthird reduction process may be due to further reduction of the ring

^cnot observed

configurations) with input parameter from structural data. It is found that the calculated $S_0 \rightarrow S_1$ transition energies agree well with the experimental values. The presence of more than one nitro group in the peripheral position of the porphyrin results in the large CI in which the excited singlet and triplets are almost isoenergetic. The effect of nitro group substitution in the pyrrole carbons is well pronounced in the electrochemical redox data of these porphyrins.

3.3 Electrochemical redox studies

The CV data of the free-base porphyrins and their copper(II) derivatives are presented in table 3. The potentials reported here are all reversible involving π -ring, one-electron oxidation/reduction. In a few cases, it is found that third reduction occurs at a more cathodic potential and this possibly involves nitro group reduction. It is seen that substitution of nitro groups leads to easier reduction of the porphyrin ring and relatively difficult ring oxidation. A comparison of the relative magnitude of the shifts in these potentials with increasing substitution of the number of nitro groups in the porphyrin reveals the following. The free-base dinitrotetraphenylporphyrins are relatively easier to reduce by 450–600 mV and the corresponding trinitro derivatives by 600–750 mV relative to the unsubstituted tetraphenylporphyrin (H_2 TPP), while the first and second ring oxidations are found to be more difficult by \approx 180 mV and 250 mV respectively. The copper(II) derivatives of these nitroporphyrins display similar electrochemical redox behaviour as those observed for the free-base porphyrins. The shifts

in the first and second ring reductions are about 570 and 700 mV respectively, while the shifts in the corresponding ring oxidations are found to be 200 and 300 mV respectively, with reference to CuTPP. It is of importance to note that the ring redox potentials are isomer specific depending on the location of nitro groups in the different pyrrole carbons. The AM1 calculations on the different isomers of the free-base nitroporphyrins afford a possible reason for the variation in the redox potential data in these systems. In general, the magnitude of electrochemical redox potentials of the porphyrins are related to the relative energy levels of HOMO/LUMO assuming that the energetics of the solvent and other contributions remain invariant¹⁹. The observation that the ring reductions are more sensitive to the substitution of the nitro groups in the pyrrole carbons of the porphyrins suggest that the perturbations in the energy levels of the LUMO in different isomers is dominant. It is found that the first ring reduction potentials bear a direct relationship with the energy levels of the LUMO in different isomers of dinitro porphyrins (figure 4). The variation of the first ring reductions observed for the dinitroporphyrins indicates that the isomers *a* and *b* are relatively easier to reduce compared to *c*, *d* and *e*. This is rationalised as follows: The two LUMO's c_1 and c_2 in the unsubstituted porphyrin under D_{4h} symmetry have large orbital coefficient on the pyrrole carbons, meso carbons and nitrogens of the opposite pyrrole rings. The presence of nitro groups at the pyrrole carbons situated in the opposite pyrrole rings leads to stabilisation of c_2 (LUMO) relative to c_1 (LUMO + 1) leading to the easier reduction in the isomer *a* and *b*. This is in excellent agreement with the observed shift in the potentials of *a* and *b* relative to H_2 TPP. On the other hand, substitution of nitro groups in the adjacent pyrrole rings (see isomers *c*, *d* and *e*) leads to the stabilisation of both c_1 and c_2 . This is manifested in the observation of more cathodic ring reduction for the isomers *c*, *d* and *e*. The small variation in the magnitude of the potential among *c*, *d* and *e* implies the different extents to which c_1 and c_2 are stabilised in these isomers.

3.4 X-ray crystal structure

The molecule 3, 7, 13 trinitro 5, 10, 15, 20- tetraphenylporphyrinatocopper(II) crystallised in triclinic system. The bond length, bond angles and dihedral angles are given in tables 4, 5 and 6. The pluto diagram with the atom labeling scheme for the porphyrin molecule is given in figure 5a. The three nitro groups are found to be in 3, 7 and 13 positions of the pyrrole rings. The porphyrin molecule is found to be slightly distorted with an average deviation of 0.14 Å from the mean N_4 plane and an average deviation of 0.14 Å as well as from the CuN_4 plane (the plane passing through the Cu atom and four nitrogen atoms of the pyrrole rings). The perpendicular deviation of the atoms of the porphyrin core from the mean N_4 plane is shown in figure 5b. The displacement of the pyrrole rings alternately up and down with respect to the N_4 plane gives rise to 'saddle' conformation of the porphyrin core. The meso carbon atoms C5, C10, C15 and C20 are displaced by 0.12, - 0.18, - 0.21 and 0.01 Å from the mean N_4 plane. The nitro groups of the pyrrole ring labelled A, B and C make an angle of 42.0°, 59.03° and 54.12° respectively, with the mean N_4 plane and are tilted by an angle of 32.30°, 54.16° and 50.64° respectively, with the individual pyrrole rings. The nitrogen atom of the nitro groups are displaced by - 0.18, 0.36 and 0.27 Å respectively, from the plane of the pyrrole rings A, B and C. It is observed that the unsubstituted pyrrole ring shows the least deviation from the mean plane and is tilted by an angle of 3.44° with respect to the

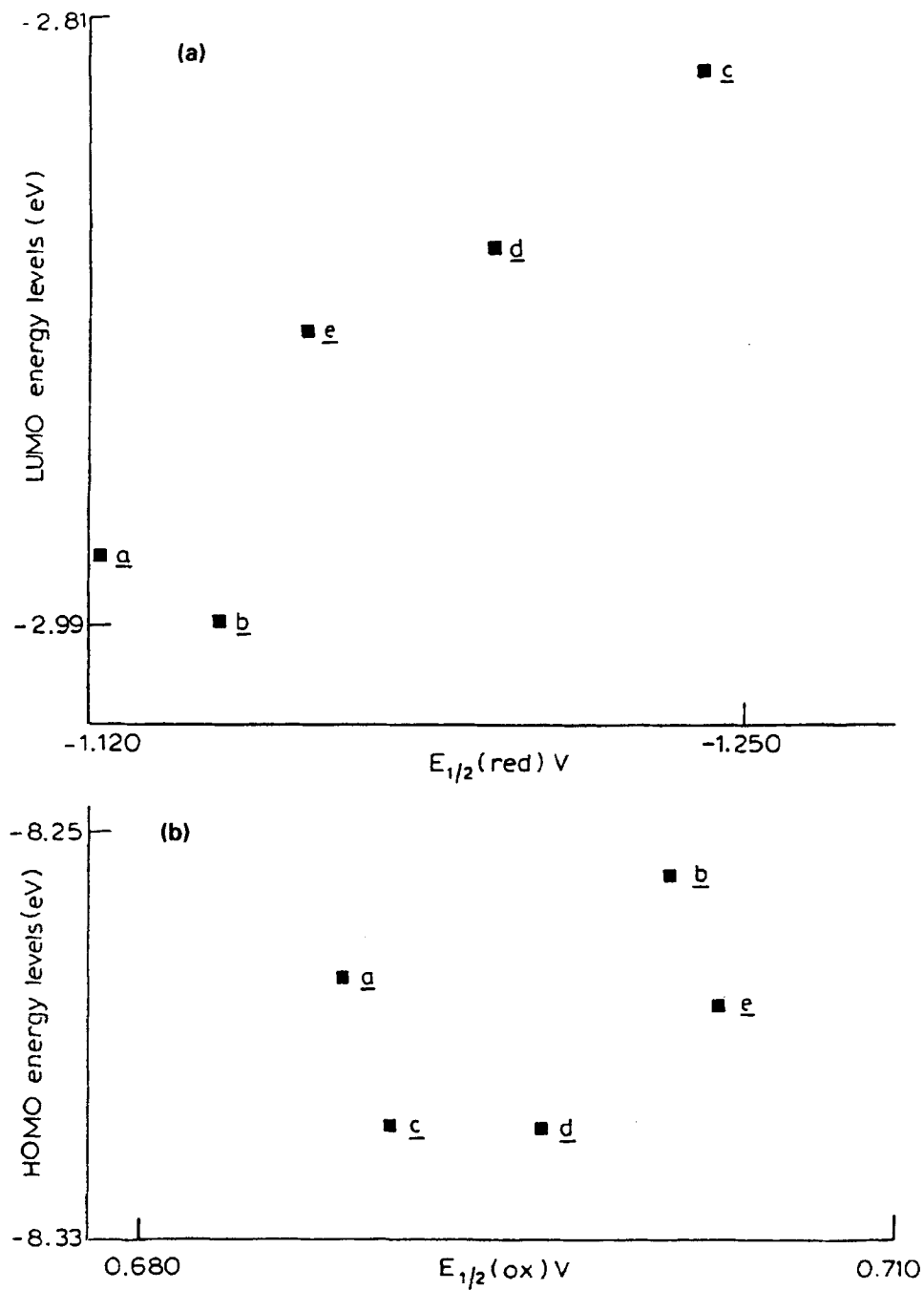


Figure 4. Plots of theoretically obtained HOMO/LUMO energy levels of free-base dinitrotetraphenylporphyrin versus $E_{1/2}(\text{ox})/E_{1/2}(\text{red})$ potential obtained from electrochemical measurements.

Table 4. Bond distances of non-hydrogen atoms of the isomer 3, 7, 13 trinitrocopper(II)tetraphenylporphyrin in Å

CU1–N21	2.10(2)	C14–C15	1.38(3)
CU1–N24	1.96(2)	C15–C16	1.36(3)
CU1–N22	2.01(2)	C16–C17	1.42(3)
CU1–N23	1.95(2)	C17–C18	1.37(3)
N21–C1	1.33(2)	C18–C19	1.46(3)
N21–C4	1.38(3)	C19–C20	1.37(3)
N22–C9	1.33(3)	C5–C51	1.55(3)
N22–C6	1.45(3)	C51–C52	1.41(3)
N23–C14	1.44(2)	C51–C56	1.34(3)
N23–C11	1.41(2)	C52–C53	1.39(3)
N24–C19	1.39(3)	C53–C54	1.34(3)
N24–C16	1.43(3)	C54–C55	1.40(3)
C1–C2	1.46(3)	C55–C56	1.40(3)
C1–C20	1.40(3)	C10–C101	1.47(3)
C2–C3	1.34(3)	C101–C102	1.34(3)
C3–C4	1.39(3)	C101–C106	1.40(3)
N31–C3	1.42(3)	C102–C103	1.40(3)
N31–O31	1.20(2)	C103–C104	1.31(3)
N31–O32	1.22(2)	C104–C105	1.38(3)
C4–C5	1.41(3)	C105–C106	1.42(3)
C5–C6	1.38(3)	C15–C151	1.51(3)
C6–C7	1.45(3)	C151–C156	1.33(3)
C7–C8	1.36(3)	C151–C152	1.40(3)
C7–N71	1.46(3)	C152–C153	1.43(3)
N71–O72	1.19(2)	C153–C154	1.35(3)
N71–O71	1.24(3)	C154–C155	1.38(3)
C8–C9	1.46(3)	C155–C156	1.44(3)
C9–C10	1.41(3)	C20–C201	1.48(3)
C11–C10	1.38(3)	C201–C202	1.42(3)
C11–C12	1.43(3)	C201–C206	1.32(3)
C12–C13	1.35(3)	C202–C203	1.38(3)
C13–C14	1.44(3)	C203–C204	1.34(3)
C13–N131	1.49(3)	C204–C205	1.36(3)
N131–O131	1.20(2)	C205–C206	1.45(3)
N131–O132	1.23(2)		

mean plane. The other pyrrole rings make an angle of 8.58°, 9.95° and 7.11° and shows large deviation from the mean plane. The 'saddle' type conformation of the substituted pyrrole ring must arise due to steric interaction between the nitro group and the neighbouring phenyl groups.

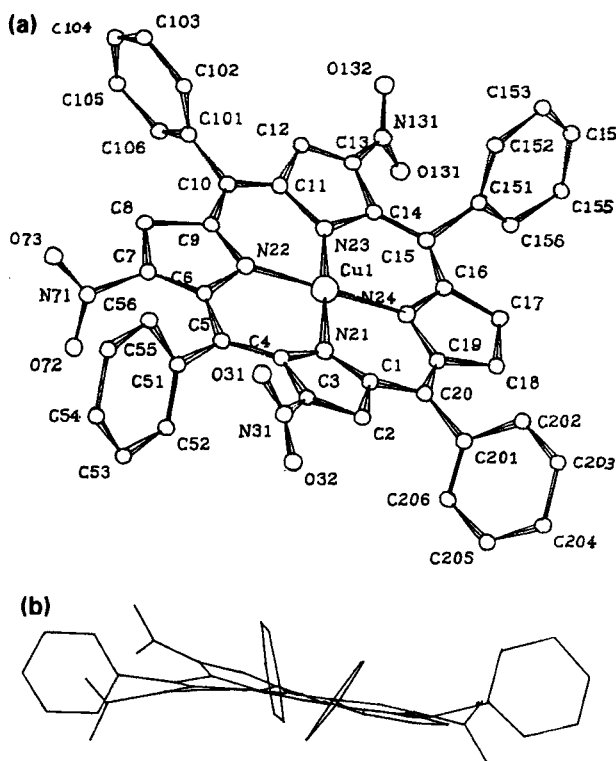
It is recognised that substitution of organic functional groups at the pyrrole carbons of H₂TPP leads to the distortion of the planer porphyrin core²⁰. The important question that arises is the critical number of the substituents that may be necessary to induce the deviation of the planarity of the porphyrin core. It is found that the substitution of eight groups, phenyl¹, bromine² and ethyl²¹ results in severe distortion of the core. The same feature is observed on methylation of one of the nitrogens²². In one of the ongoing studies we found mono methylation of one of the pyrrole carbons of H₂TPP does not result in any deviation of the planar core (Sen and Krishnan, unpublished). We believe from these studies that a minimum number of substituents

Table 5. Bond angles of non-hydrogen atoms of the isomer 3, 7, 13 trinitricopper(II) tetraphenylporphyrin

C1–N21–C4	105(2)	C14–C15–C151	114(2)
C1–N21–CU1	126(2)	C16–C15–C151	117(2)
C4–N21–CU1	129(2)	C11–C10–C9	122(2)
N21–C1–C1	111(2)	C11–C10–C101	117(2)
N21–C1–C20	128(2)	C9–C10–C101	121(2)
C2–C1–C20	121(2)	C19–N24–C16	104(2)
C3–C2–C1	105(2)	C19–N24–CU1	129(2)
C2–C3–N31	120(2)	C16–N24–CU1	128(14)
C2–C3–C4	108(2)	C15–C16–C17	126(2)
N31–C3–C4	131(2)	C15–C16–N24	124(2)
C5–C4–N21	122(2)	C17–C16–N24	110(2)
C5–C4–C3	127(2)	C16–C17–C18	109(2)
N21–C4–C3	110(2)	C17–C18–C19	105(2)
C4–C5–C6	126(2)	N24–C19–C20	125(2)
C4–C5–C51	117(2)	N24–C19–C18	112(2)
C6–C5–C51	117(2)	C20–C19–C18	123(2)
C5–C6–C7	130(2)	C19–C20–C1	122(2)
C5–C6–N22	125(2)	C19–C20–C201	121(2)
C7–C6–N22	105(2)	C1–C20–C201	117(2)
C8–C7–C6	112(2)	O131–N131–O132	128(3)
C8–C7–N71	118(2)	O131–N131–C13	118(2)
C6–C7–N71	1290(2)	O132–N131–C13	114(2)
O73–N71–O72	123(2)	C56–C51–C52	122(2)
O73–N71–C7	118(2)	C56–C51–C5	121(2)
O72–N71–C7	117(2)	C52–C51–C5	117(2)
C7–C8–C9	104(2)	C53–C52–C51	118(2)
C9–N22–C6	107(2)	C54–C53–C52	118(2)
C9–N22–C1	128(2)	C55–C54–C53	125(3)
C6–N22–CU1	124(2)	C54–C55–C56	116(3)
N22–C9–C10	128(2)	C51–C56–C55	120(2)
N22–C9–C8	113(2)	C102–C101–C106	118(2)
C10–C9–C8	120(2)	C102–C101–C10	121(2)
C10–C11–N23	125(2)	C106–C101–C10	121(2)
C10–C11–C12	123(2)	C101–C102–C103	123(3)
N23–C11–C12	112(2)	C102–C103–C104	119(3)
C13–C12–C11	105(2)	C105–C104–C103	122(3)
C12–C13–C14	112(2)	C104–C105–C106	119(3)
C12–C13–N131	121(2)	C101–C106–C105	118(2)
C14–C13–N131	127(2)	C156–C151–C152	118(2)
N24–CU1–N22	180(4)	C156–C151–C15	122(2)
N24–CU1–N23	91(7)	C152–C151–C15	120(2)
N22–CU1–N23	89(7)	C151–C152–C153	120(2)
N24–CU1–N21	90(7)	C154–C155–C156	117(2)
N22–CU1–N21	90(8)	C154–C153–C152	120(3)
N23–CU1–N21	178(8)	C153–C154–C155	122(2)
O31–N31–O32	122(2)	C151–C156–C155	124(3)
O31–N31–C3	119(2)	C206–C201–C202	117(2)
O32–N31–C3	118(2)	C206–C201–C20	122(2)
C11–N23–C14	105(2)	C202–C201–C20	121(2)
C11–N23–CU1	128(14)	C203–C202–C201	120(2)
C14–N23–CU1	126(14)	C204–C203–C202	122(3)
C15–C14–N23	123(2)	C203–C204–C205	120(3)
C15–C14–C13	130(2)	C204–C205–C206	118(3)
N23–C14–C13	106(2)	C201–C206–C205	123(3)
C14–C15–C16	127(2)		

Table 6. Selected torsional angles for the isomer 3, 7, 13 trinitrocopper(II) tetraphenylporphyrin

C4–N21–Cu1–N22	–9(2)	C1–N21–Cu1–N22	–175(2)
C4–N21–Cu1–N24	172(3)	C1–N21–Cu1–N24	6(2)
N21–C1–C20–C201	–171(3)	C2–C1–C20–C201	6(4)
C1–C2–C3–N31	–171(3)	C2–C3–N31–O31	133(3)
C2–C3–N31–O32	–42(5)	N31–C3–C4–N21	171(3)
C4–C3–N31–O3	–37(5)	C4–C31–N31–O32	148(3)
N31–C3–C4–C5	–24(5)	C3–C4–C5–C51	0.48(5)
N21–C4–C5–C51	164(3)	C51–C5–C6–C7	–2(5)
C51–C5–C6–N22	178(3)	N23–C11–C10–C101	–179(3)
C12–C11–C10–C101	–1(4)	C11–C12–C13–N131	171(2)
C12–C13–N131–O131	–127(3)	C12–C13–N131–O132	50(4)
N131–C13–C14–C15	14(5)	N131–C13–C14–N23	–167(3)
C14–C13–N131–O132	–135(3)	C14–C13–N131–O131	48(4)
C8–C9–C10–C101	11(5)	N22–C9–C10–C101	–172(3)
C13–C14–C15–C151	17(5)	N23–C14–C15–C151	–162(2)
C151–C15–C16–C17	–19(5)	C151–C15–C16–N24	156(3)
N22–C6–C7–N71	163(3)	C5–C6–C7–N71	–17(5)
N71–C7–C8–C9	–167(3)	C6–C7–N71–O72	–50(5)
C6–C7–N71–O73	140(3)	C8–C7–N71–O73	–49(4)
C8–C7–N71–O72	122(3)	N24–C19–C20–C201	–177(3)
C18–C19–C20–C201	–8(5)		

**Figure 5.** (a) Pluto diagram of copper(II) derivative of 3, 7, 13-trinitrotetraphenylporphyrin with atom labelling scheme (b) Edge on view showing saddle conformation.

that may be necessary to distort the planar core is two. Another fact that emerges is the Van der Waal's radius of the substituent. The distortion apparently arises from the steric constraints imposed by the substituents on the orientation of the meso phenyl groups. Hence, larger the Van der Waal's radius of the substituent, greater would be the steric restraint leading to permanent deviation of the planar core. The bromine and triatomic nitro group have almost the same Van der Waal's radius and it is expected that these substituents would cause steric constraints. The distortion of the planar porphyrin core leads to manifestation of many unusual properties.

The AM1 calculations performed on these distorted systems revealed large perturbation of HOMO/LUMO energy levels. In addition, this distortion also results in the widely different coefficients of electron density on the pyrrole, meso carbons and imino nitrogens. Generally, the effects brought about by distortion of the porphyrin core is clearly manifested in the basicity values of imino nitrogens, increased rates of metallation, varying electrochemical redox potentials, shift in the singlet transition energies ($S_0 \rightarrow S_1$) and interesting triplet absorption spectra.

Acknowledgement

The author thank the Department of Science and Technology, Government of India, New Delhi, for financial support.

References

1. Medforth C J, Senge M O, Smith K M, Sparks L D and Shelnut J 1992 *J. Am. Chem. Soc.* **114** 9859
2. Bhyrappa P and Krishnan V 1991 *Inorg. Chem.* **30** 239
3. Rao S and Krishnan V 1994 *J. Mol. Struct.* **327** 279
4. Tsuchiya S 1991 *J. Chem. Soc., Chem. Commun.* 716
5. Dahal S, Nethaji M and Krishnan V 1994 *Acta Crystallogr.* **C50** 314
6. Dahal S and Krishnan V 1995 *J. Photochem. Photobiol. A: Chem.* **89** 105
7. Bartoli J F, Battioni P, De Foor W R and Mansuy D 1994 *J. Chem. Soc., Chem. Commun.* 23
8. Baldwin J E, Crossley M J and Debernardis 1982 *Tetrahedron* **39** 685
9. Catalano M M, Crossley M J, Harding M M and King L C 1984 *J. Chem. Soc., Chem. Commun.* 1533
10. Hombrecher H K, Gherdan V M, Ohm S, Cavaleiro J A S, Neves M G P M S and Condesso M F 1993 *Tetrahedron* **49** 8569
11. Vicente M G H, Neves M G P M S, Cavaleiro J A S, Hombrecher H K and Koll D 1996 *Tetrahedron Lett.* **37** 261
12. Alder O D, Longo F R, Kampas F and Kim J 1970 *J. Inorg. Nucl. Chem.* **32** 2443
13. D'Souza F and Krishnan V 1990 *Inorg. Chim. Acta* **176** 131
14. Sheldrick G M 1985 *SHELXS86: Program for the solution of crystal structure*, Univ. of Gottingen, Germany
15. Sheldrick G M 1993 *SHELXL93, Program for the refinement of crystal structures*, Univ. of Gottingen, Germany
16. Crossley M J, Field L D, Harding M M and Sternhell S 1987 *J. Am. Chem. Soc.* **109** 2335
17. Dahal S and Krishnan V 1997 *Chem. Phys. Lett.* **274** 390
18. Gouterman M J 1959 *Chem. Phys.* **30** 1139
19. Kadish K M 1986 *Prog. Inorg. Chem.* **34** 435
20. Senge M O 1992 *J. Photochem. Photobiol. B: Biol* **16** 3
21. Barkigia K M, Berber M D, Fajer J, Medforth C J, Renner M W and Smith K M 1990 *J. Am. Chem. Soc.* **112** 8851
22. Anderson O D, Kapelaue A B and Lavalley D K 1980 *Inorg. Chem.* **19** 2101
23. Giraudeau A, Callot H J, Jordan J, Ezhar I and Gross M 1979 *J. Am. Chem. Soc.* **101** 3857